# A Proposed Algorithm for Moisture Fluxes from Atmospheric Rivers

YONG ZHU AND REGINALD E. NEWELL

*Department of Earth, Atmospheric and Planetary Sciences, Massachusetts Institute of Technology, Cambridge, Massachusetts*

## ABSTRACT

A new algorithm is applied to study water vapor fluxes in the troposphere using wind and moisture data from the European Centre for Medium-Range Weather Forecasts. The fluxes are divided into filamentary structures known as tropospheric rivers and what are termed here broad fields. The results show that the tropospheric rivers may carry essentially the total meridional transport observed in the extratropical atmosphere but may occupy only about 10% of the total longitudinal length at a given latitude. The transient fluxes in traditional studies do not catch the filamentary structures completely and may therefore underestimate the fraction of transport assigned to moving systems, as well as omitting the geographical concentration. The mean flow and eddy fluxes evaluated by the new algorithm are considered to be more physically realistic.

## 1. Introduction

Traditionally, the transport of water vapor in the atmosphere has been studied by classifying the fluxes into the components contributed by time and zonal mean flows, stationary eddies, and transient perturbations. According to Peixoto and Oort (1992), ". . . the transport is mainly accomplished by baroclinic lows associated with the polar front and by stationary eddies, such as subpolar lows and subtropical anticyclones, together with their transient pulsations." But exactly how do the baroclinic eddies transport the water vapor, and how large is the transport by the different types of disturbances? The Norwegian classical cyclone model was established without considering the dynamic and energetic effect of moisture. There appear to be no statistical estimates of the global transport of water vapor by baroclinic cyclones by themselves.

The transient perturbations are usually separated from the effects of so-called mean circulations by the following convention, originally put forward by Reynolds (1894) for turbulence studies and extensively used in the 1950s–1970s by, for example, Starr and Peixoto (1971) for water vapor. If $q$, $u$, and $v$ represent specific humidity, zonal wind, and meridional wind components at a particular longitude $\lambda$ and latitude $\phi$, they may be resolved as follows into mean and transient components:

$$q_{\lambda,\phi} = \overline{q}_{\lambda,\phi} + q'_{\lambda,\phi} \tag{1a}$$

$$u_{\lambda,\phi} = \overline{u}_{\lambda,\phi} + u'_{\lambda,\phi} \tag{1b}$$

$$v_{\lambda,\phi} = \overline{v}_{\lambda,\phi} + v'_{\lambda,\phi}, \tag{1c}$$

where the overbar represents the time average,

$$\overline{A} = \frac{1}{T} \int_0^T A \, dt, \tag{2}$$

and the prime represents the deviation from the time mean. Then by cross-multiplication and further use of the definition of time average, one obtains the zonal and meridional fluxes as

$$\overline{qu} = \overline{q}\,\overline{u} + \overline{q'u'} \tag{3a}$$

and

$$\overline{qv} = \overline{q}\,\overline{v} + \overline{q'v'}, \tag{3b}$$

wherein the total transport on the lhs is expressed in terms of that by time mean motions and so-called transient perturbations.

A further convention that is often used is to express the various quantities as departures from their zonal mean values as follows:

$$q_{\lambda,\phi} = [q]_\phi + q^*_{\lambda,\phi}, \tag{4}$$

similarly for $u$ and $v$, where the square bracket represents the zonal mean at a given latitude,

$$[A]_\phi = \frac{1}{2\pi} \int_0^{2\pi} A \, d\lambda, \tag{5}$$

and the asterisk represents the deviation from the zonal mean at a given longitude.

Proceeding as for Eqs. (3), and but using (5) instead of (2) and taking time averages first, one obtains

*Corresponding author address:* Yong Zhu, Dept. of Earth, Atmospheric and Planetary Sciences, Massachusetts Institute of Technology, Room 54-1822, 77 Massachusetts Ave., Cambridge, MA 02139.

$$[\overline{qu}] = [\overline{q}][\overline{u}] + [\overline{q'u'}] + [\overline{q^*\overline{u}^*}] \tag{6a}$$

and

$$[\overline{qv}] = [\overline{q}][\overline{v}] + [\overline{q'v'}] + [\overline{q^*\overline{v}^*}], \tag{6b}$$

where the three components on the rhs are transports by the time and zonal mean motions, the transient perturbations, and the so-called stationary eddies. An example of the latter is the positive value contributed by the association between moist air moving poleward in the western Atlantic and dry air moving equatorward in the eastern Atlantic, a circulation accompanying the mean subtropical high pressure system.

The vertical integrals of the transport components in the zonal ($\lambda$) and meridional ($\phi$) directions are

$$\overline{Q}_\lambda = \frac{1}{g} \int_{P_0}^{300\,\text{hPa}} \overline{qu}\ dp \tag{7a}$$

$$\overline{Q}_\phi = \frac{1}{g} \int_{P_0}^{300\,\text{hPa}} \overline{qv}\ dp, \tag{7b}$$

where $p_0$ is surface pressure and 300 hPa is taken as the pressure limit at the highest altitude of reliable radiosonde measurements.

In Eqs. (7), it is customary to substitute (6) and treat the total flux over a time period, such as a month or more, as the sums of contributions by the time and zonal mean motions, transient perturbations, and stationary eddies. There are a number of ways of performing these resolutions of atmospheric fluxes, and the physical processes involved are included in some of the discussions (e.g., Starr and White 1952a,b).

Substituting (3) in (7) yields

$$\overline{Q}_\lambda = \frac{1}{g} \int_{P_0}^{300\,\text{hPa}} \overline{q}\,\overline{u}\ dp + \frac{1}{g} \int_{P_0}^{300\,\text{hPa}} \overline{q'u'}\ dp \tag{8a}$$

and

$$\overline{Q}_\phi = \frac{1}{g} \int_{P_0}^{300\,\text{hPa}} \overline{q}\,\overline{v}\ dp + \frac{1}{g} \int_{P_0}^{300\,\text{hPa}} \overline{q'v'}\ dp. \tag{8b}$$

Using $\mathbf{Q} = \mathbf{i}Q_\lambda + \mathbf{j}Q_\phi$, where $\mathbf{i}$ is a unit vector eastward and $\mathbf{j}$ a unit vector northward, gives

$$\overline{\mathbf{Q}} = \mathbf{i}\overline{Q}_\lambda + \mathbf{j}\overline{Q}_\phi \tag{9a}$$

and

$$\mathbf{Q}' = \mathbf{i}\frac{1}{g} \int_{P_0}^{300\,\text{hPa}} \overline{q'u'}\ dp + \mathbf{j}\frac{1}{g} \int_{P_0}^{300\,\text{hPa}} \overline{q'v'}\ dp, \tag{9b}$$

from the second terms of Eqs. (8a) and (8b).

Gridpoint data from the European Centre for Medium-Range Weather Forecasts (ECMWF) for wind velocity and relative humidity (converted to specific humidity) for levels of 1000, 850, 700, 500, 400, and 300 hPa and daily data for times of 0000 and 1200 UTC are used throughout this study. For the period after January 1992, the 925-hPa level was also included.

The data were used to evaluate $\overline{\mathbf{Q}}$ and $\mathbf{Q}'$ for a July sample containing the years 1991, 1994, and 1995, as these data were locally available. The $\overline{\mathbf{Q}}$ map shown in Fig. 1a shows the mean flow from Eq. (9a) is mostly zonal in the Tropics, with substantial meridional components between 35° and 55°N in the North Atlantic and North Pacific, as well as south of Australia, southeast of South America, and in the southeast Pacific. There is a strong concentrated interhemispheric flow into the Arabian Sea. The $\mathbf{Q}'$ map shows that transient perturbations from Eq. (9b) for the same period (Fig. 1b) are mostly poleward between 20°–70°S and 35°–60°N, particularly over the ocean.

It is well known that there is a large amount of water vapor transport in the region of the Asian summer monsoon. The daily maps show large changes in the water vapor flux vectors every day over these areas; the persistent monsoon circulations are supported by transient filamentary water vapor fluxes and other disturbances on a scale less than that of the monsoon system. These features, while transient, do not show on the $\mathbf{Q}'$ map of Fig. 1b. In fact, Fig. 1b shows that these regions were especially quiet in this monsoon season for the three Julys selected and that in this particular resolution, most of the flux is by the mean flow $\overline{\mathbf{Q}}$. Over the middle-latitude oceans, the transient $\mathbf{Q}'$ perturbations are almost uniformly poleward, essentially down the water vapor mixing ratio gradient; they show no apparent links with the storm tracks. The water vapor flux by the mean flow $\overline{\mathbf{Q}}$ in Fig. 1a suggests that it is the mean easterly flux across the Arabian Sea and the Bay of Bengal that supplies moisture to the monsoon region; while this may be the main contributor, it is well known that the tropical storms that enter the region from the east as typhoons also contribute substantially to the precipitation in the region at this time. It has long been thought that mean motions contribute most of the water vapor flux at low latitudes (Starr and Peixoto 1971), but for this particular region they do not seem to account for all the physical phenomena involved in the transport. Hence, both the $\mathbf{Q}'$ map and the $\overline{\mathbf{Q}}$ map omit physical mechanisms thought to be important.

We showed elsewhere (Newell and Zhu 1994) that when the flux was subjected to a harmonic analysis at each grid point (spaced about 2.5° apart), and the high-frequency periods (shorter than 3 days) portion of the analysis was examined, then correspondence with storm tracks became evident over the middle-latitude oceans, and high values also occurred over the ocean near Southeast Asia. Furthermore, the magnitudes of these transports by the high frequency motions were much larger than the individual transports of Fig. 1b, even though the total flux may be the same when integrating these rather uniform vectors across an ocean. Middle-latitude oceanic values exceeded 300–400 kg m$^{-1}$ s$^{-1}$, while the values in Fig. 1b were generally about 50 kg m$^{-1}$ s$^{-1}$.

It was suggested (Newell et al. 1992) that the water vapor transport in the troposphere is characterized by a filamentary structure, called tropospheric rivers. The
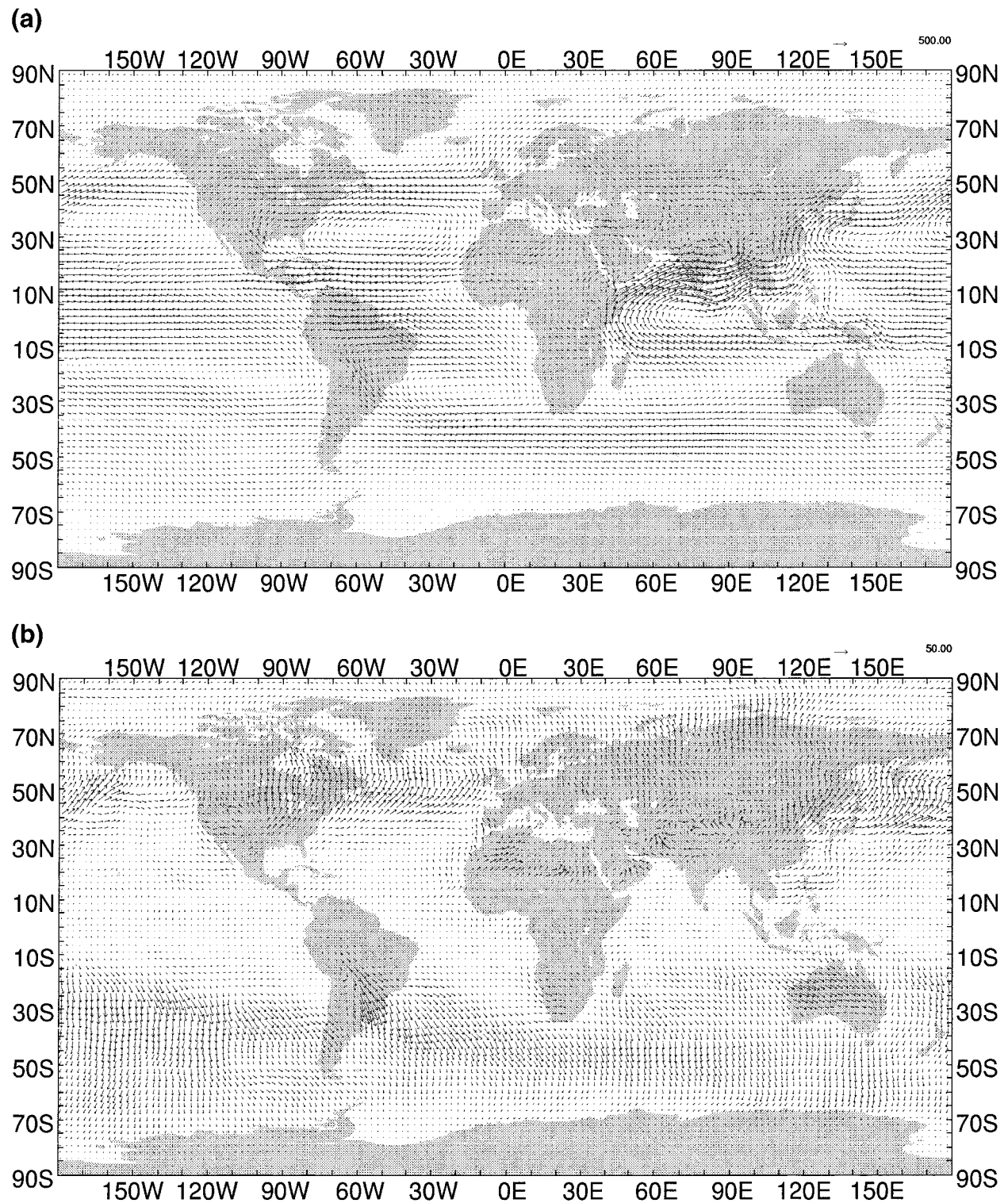
**(a)**



**(b)**



Fig. 1. (a) Average values of the mean moisture transport (kg m$^{-1}$ s$^{-1}$) from Eq. (9a) for July 1991, 1994, and 1995. Sample vector magnitude $|\overline{\mathbf{Q}}'|$ illustrated in upper-right corner. (b) Average values of the transient eddy moisture transport (kg m$^{-1}$ s$^{-1}$) from Eq. (9b) for July 1991, 1994, and 1995. Sample vector magnitude $|\mathbf{Q}'|$ illustrated in upper-right corner.

moisture flux in a typical tropospheric river is about $1.6 \times 10^8$ kg s$^{-1}$, which is similar to the flux in the Amazon River. The evaluation of Peixoto and Oort (1992) showed that the zonally averaged annual mean meridional water vapor flux poleward across 30°N is about $7 \times 10^8$ kg s$^{-1}$. Thus, four or five atmospheric rivers in each hemisphere may carry the majority of the meridional fluxes over the globe.

To try to assess the magnitude of the river fluxes in the troposphere, we introduce a new approach in the present study by dividing the fluxes into river fluxes and the residual called the broad fluxes.

## 2. Partition of water vapor fluxes

A comparison of Fig. 1b above and Fig. 1 given by Newell et al. (1992) shows a major difference in the middle-latitude oceanic fluxes, with the traditional approach (Fig. 1b) smoothing out the influence of the filamentary structure evident in Fig. 1. This difference is important when relating the daily water vapor fluxes to storm tracks, cold frontal positions, and so on. The relationship between rivers and cold-frontal positions is discussed by Newell and Zhu (1994). The problem becomes how best to set up an analysis technique that properly encompasses the filamentary structure in atmospheric water vapor transport fields. This was approached by sorting the fluxes at each point along a given latitude into two groups: those exceeding a certain limit related to the mean value at a given latitude (the rivers), and the rest, called the broad fluxes. The total flux at a point is given as

$$\mathbf{Q}_t = \mathbf{Q}_r + \mathbf{Q}_b, \tag{10}$$

where subscripts $t$, $r$, and $b$ indicate total, river, and broad flux, respectively. In the present study, the river fluxes are defined as the fluxes whose magnitude exceeds a certain limit given here by

$$Q_r \geq Q_{\text{mean}} + 0.3(Q_{\text{max}} - Q_{\text{mean}}), \tag{11}$$

where $Q_{\text{mean}}$ denotes the zonal mean along a given latitude of the magnitude of the flux in all directions. Here, $Q_{\text{max}}$ indicates the magnitude of the maximum flux along a given latitude, and the constant 0.3 is related to the strength of the rivers. The value of 0.3 was selected from a series of trials over the range 0.1–0.5 for the 12 October 1991 data. This value gave the best preservation of the river structure, which was shown for the same day in Newell et al. (1992). It also gave the best correspondence between the river contribution and the total northward flux for the periods December 1991–February 1992, June 1991–August 1991, and June 1991–May 1992, which were used as trial periods. This approach is simply a technique to emphasize the river contribution.

The fluxes obeying the criteria in Eq. (11) are shown in Fig. 2a. It is clear that the strongest fluxes have a filamentary form, which is why we termed

them atmospheric rivers, and that their length is several times larger than their width. They represent a fairly distinct physical phenomenon, as may also be seen in cross sections (e.g., Fig. 2 in Newell and Zhu 1994). While the rivers are generally directed poleward, the broad fluxes, which are the vector fluxes in regions where the river criterion from Eq. (11) is not met (Fig. 2b), are sometimes equatorward and, as expected, are less coherent. The integrated total fluxes for the same day can be found in the study of Newell et al. (1992). The magnitudes of the meridional components of the river and broad fluxes for 12 October 1991 are shown in Figs. 3a and 3b, and the distribution of their zonal mean with latitude is in Fig. 3c. The total river flux is about $11 \times 10^8$ kg s$^{-1}$ across 40°S, which is essentially the same as the total flux. Figure 2a shows that there were five rivers along this latitude. Therefore, the mean flux of each river for this day is about $2.2 \times 10^8$ kg s$^{-1}$, which is about 38% more than the flux by the Amazon River.

Another concept introduced here is the zonal scale of rivers, which is the ratio of the zonal extent of all rivers to the total longitudinal length along a latitude. This is evaluated from $(1/360) \, \Sigma_i \, \Delta\lambda_{ri}$, where $\Delta\lambda_{ri}$ in degrees is the longitudinal extent of each river at a given latitude. This scale may be greater than the width of rivers, as rivers do not lie meridionally in general. As shown in Fig. 3c, the scale was only about 0.1 at the latitudes where the moisture fluxes were largest.

## 3. Relation to cyclonic disturbances

The rivers in the Southern Hemisphere were related to long-wave circulations. Figure 4 gives the geopotential height at 1000 hPa for the same day as Figs. 2 and 3. The rivers were in or slightly ahead of the surface troughs. The equatorward and poleward flows on the west and east sides of the troughs, respectively, form filamentary wind shears or convergence lines over the surface. Since the equatorward flows are usually cold and dry and the poleward flows are warm and moist, the sharp contrasts of temperature and humidity may occur along the convergence lines in the lower troposphere, and the poleward moisture fluxes are stronger than the equatorward fluxes even if the opposite mass fluxes have the same intensity. The poleward fluxes formed by large-scale processes on the warm side of temperature fronts may be further intensified and narrowed by meso- and small-scale convective activities along the convergence lines. Formation of the rivers may be independent of the genesis and development of baroclinic cyclones, though the cyclonic activity may have an effect on the development of rivers. We have discussed the effect on rapidly developing cyclones elsewhere (Zhu and Newell 1994). The rivers are obviously the transient
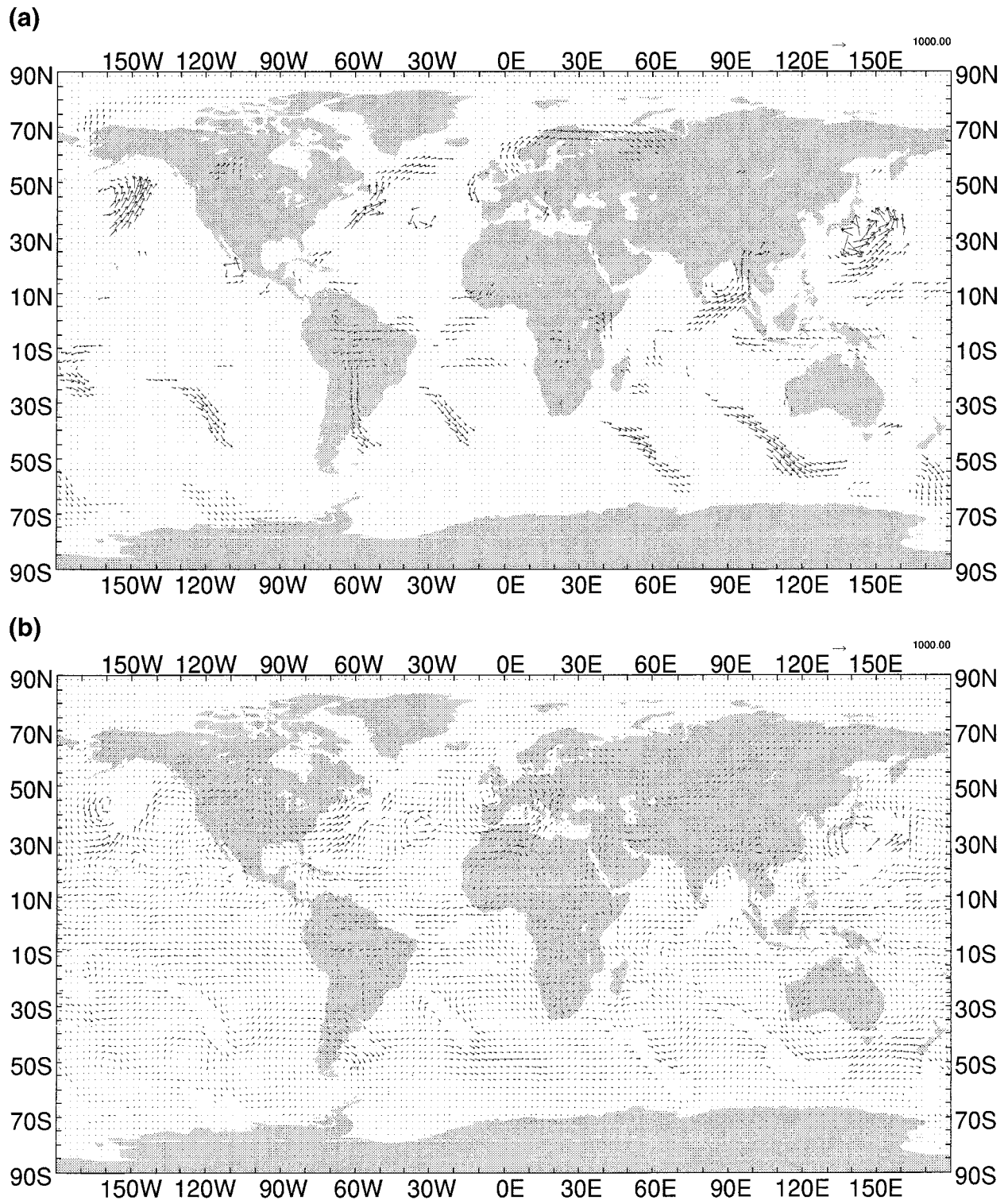
**(a)**



**(b)**



FIG. 2. (a) Moisture flux (kg m$^{-1}$ s$^{-1}$) by atmospheric rivers, isolated from the total flux using Eq. (11) for 1200 UTC 12 October 1991. Vector magnitude illustrated in upper-right corner. (b) Broad flux (kg m$^{-1}$ s$^{-1}$) corresponding to Fig. 2a using Eq. (10).
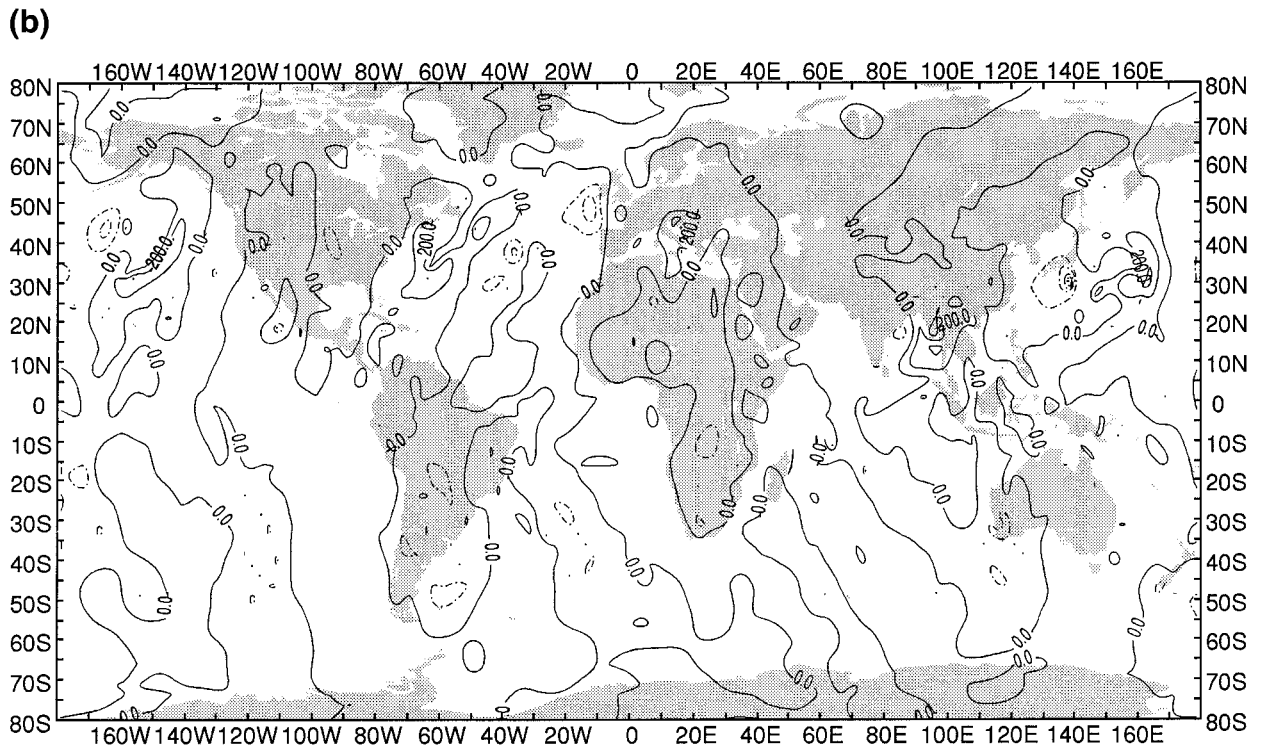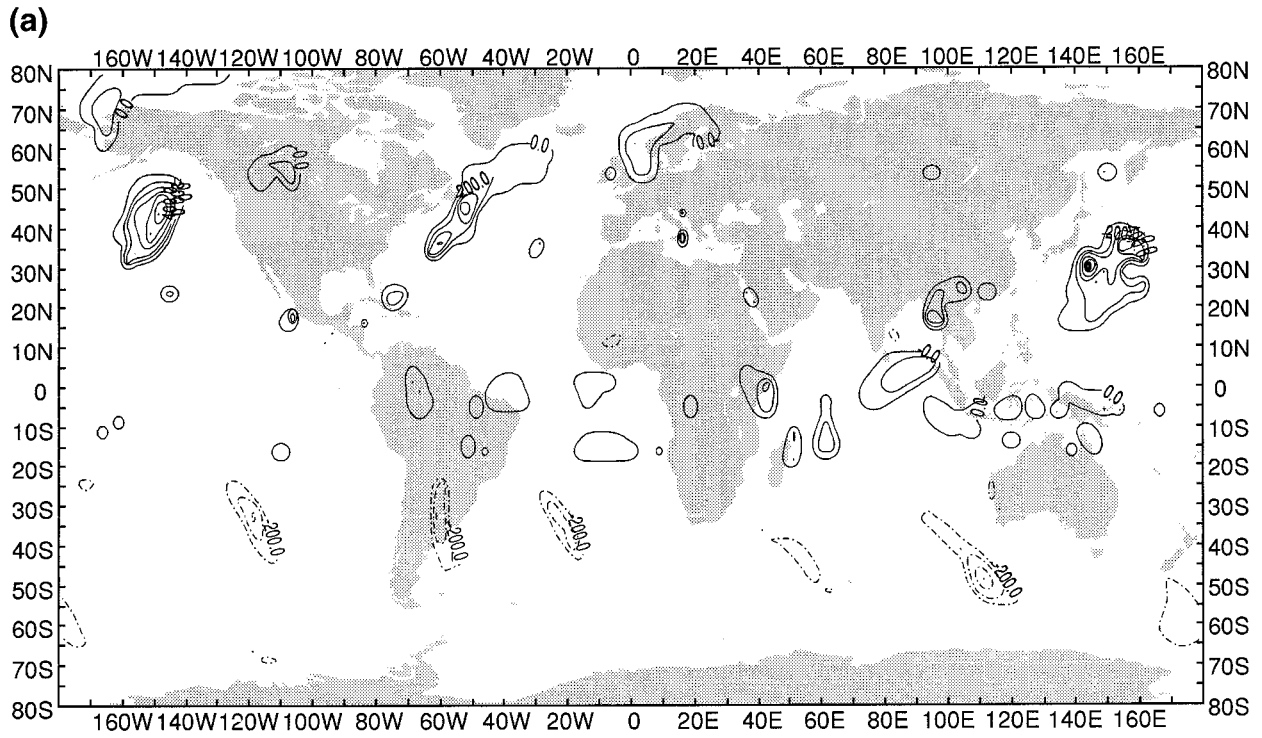
**(a)**



**(b)**



FIG. 3. (a) Meridional component of the river flux (kg m$^{-1}$ s$^{-1}$) for same data as those used for Fig. 2a. (b) Meridional component of the broad flux (kg m$^{-1}$ s$^{-1}$) for same data as those used for Fig. 2a.

**(c)**
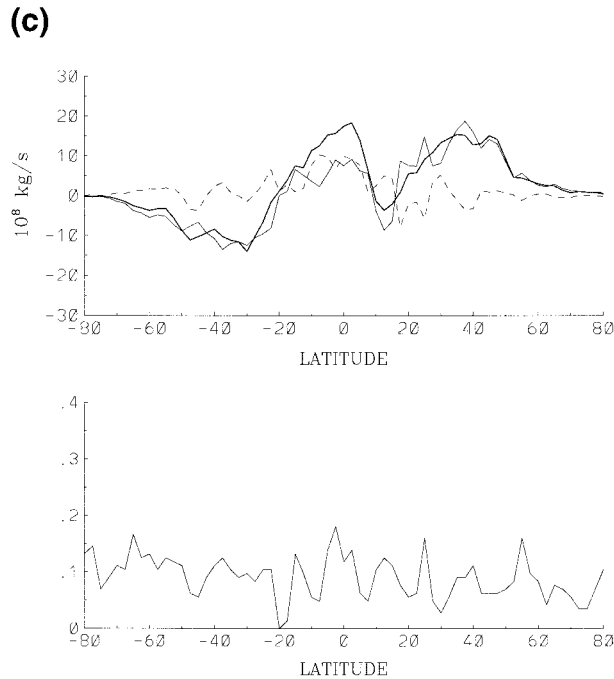


FIG. 3c. (Upper panel) Northward moisture flux by rivers, broad fluxes, and their totals for the same data as those used for Fig. 2a. Rivers, thin solid line; broad fluxes, dashed line; and total flux, thick solid line. Units are $10^8$ kg s$^{-1}$. (Lower panel) Zonal scale of rivers for same data.

circulation systems, which have an important contribution to water vapor transport.

When the baroclinic waves are destabilized, the cold and dry air behind a polar front fills up the low levels of a new cyclone. As a result, the river is pushed to the eastern edge of the cyclone and may be intensified as the wind speed increases in disturbance development. This may be seen by comparing Figs. 2a and 4. The rivers over South America, to the south of Australia, and over the northeastern Pacific were all located to the east of a cyclone. The cyclone usually moves toward the head of the river, where water vapor convergence is maximum; this point has been treated elsewhere (Zhu and Newell 1994). To the west of the cyclone centers, the flows produced equatorward moisture fluxes, as shown in Fig. 3b, in the northeast Pacific, near Japan, and near the United Kingdom. As pointed out by Zhu and Newell (1994), the extratropical cyclones over the oceans often move toward the heads of rivers. Thus, the storm tracks are located in the river tracks.

Apart from the baroclinic cyclones generated in the extratropical regions, tropical cyclones may also increase the poleward fluxes of water vapor. Figure 2a shows that Typhoon Orchid near the southeast coast of Japan produced a large poleward flux. Typhoon Pat, to the northeast, which was disappearing and merging into Orchid, produced a slightly weaker flux peak to the northeast. Since the cores of tropical cyclones are warm and moist, the maximum fluxes are closer to the storm centers, if compared with the rivers near the extratropical cyclones.
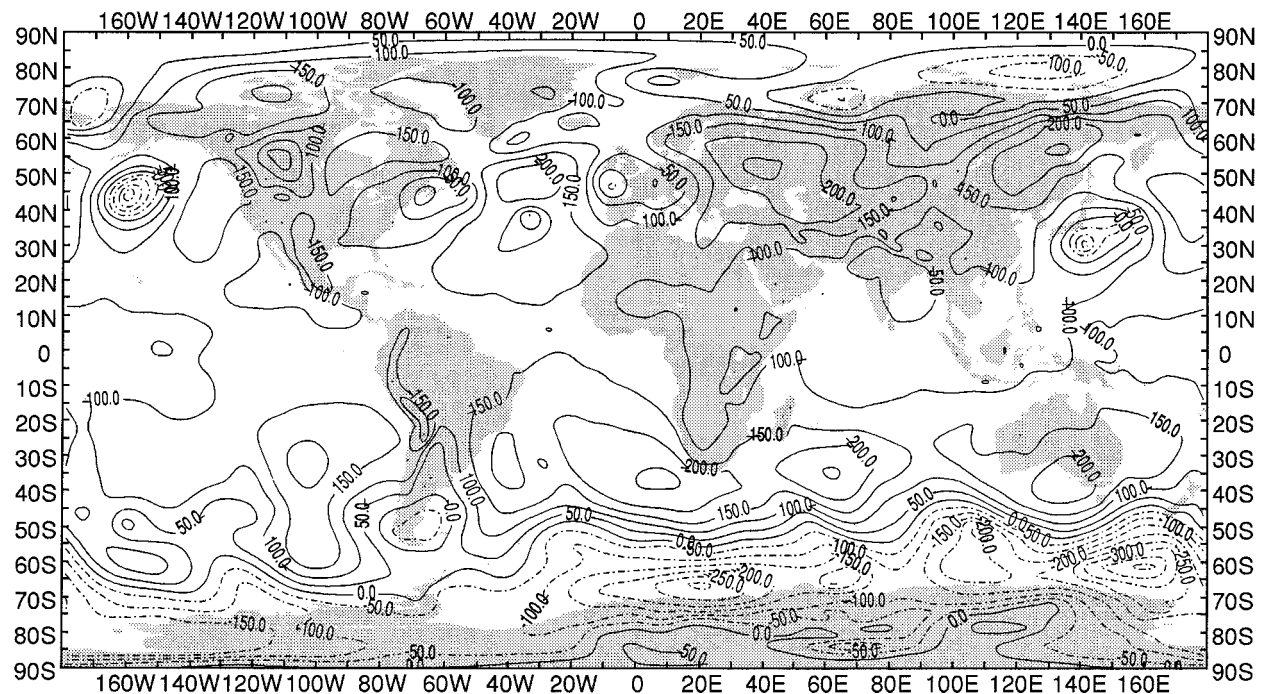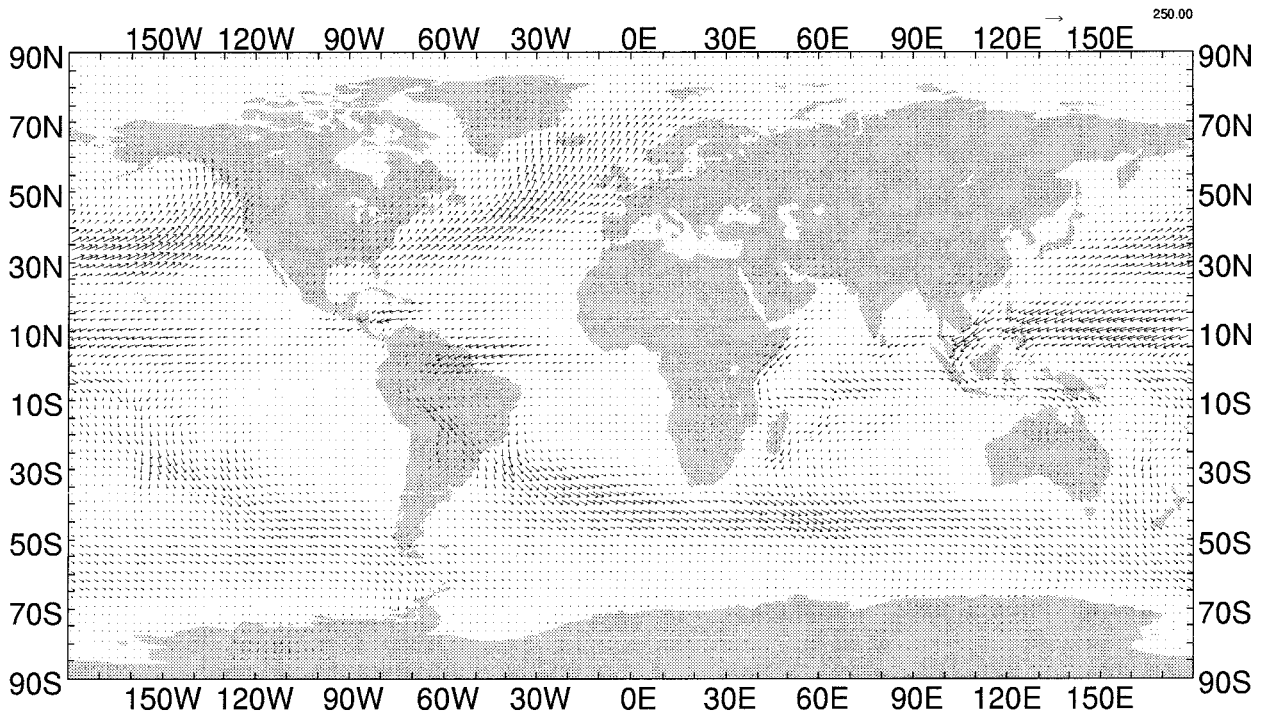


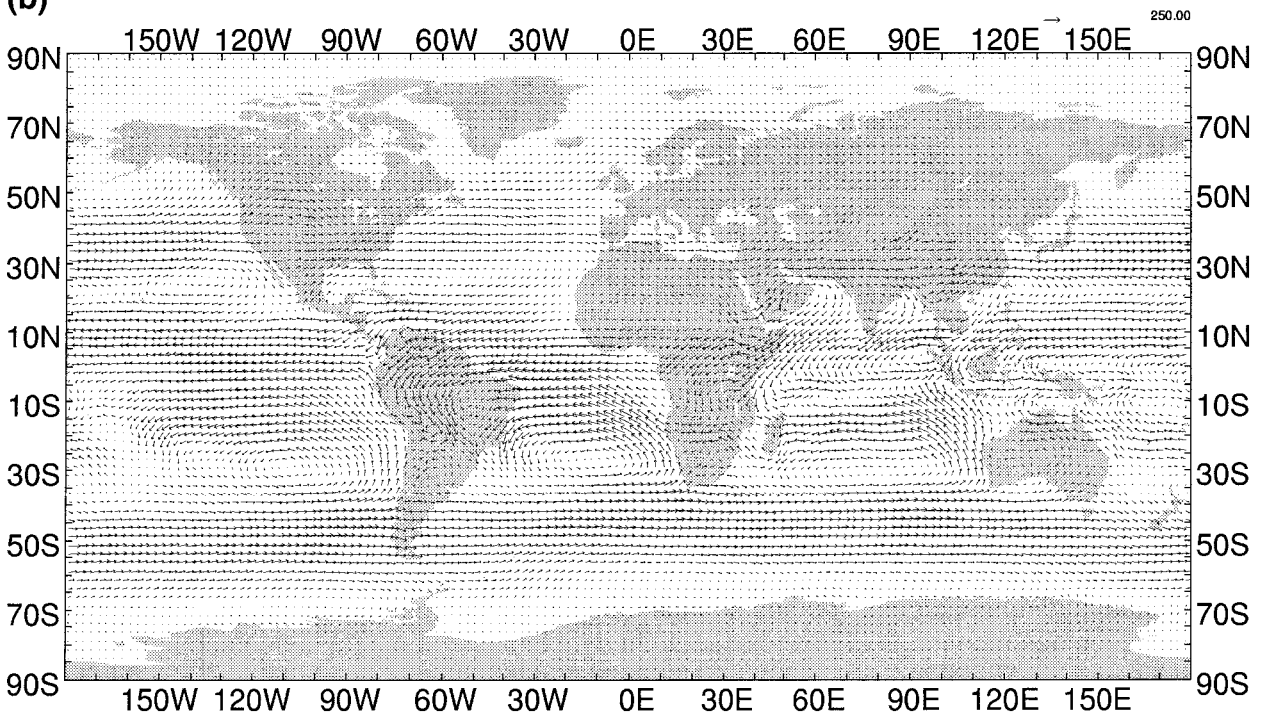FIG. 4. Geopotential height (gpm) at 1000 hPa for same data as those used for Fig. 2a.

**(a)**



**(b)**



Fig. 5. (a) River fluxes (kg m$^{-1}$ s$^{-1}$) for January 1992, 1995, and 1996. Sample vector magnitude illustrated in upper-right corner. (b) Broad fluxes (kg m$^{-1}$ s$^{-1}$) for January 1992, 1995, and 1996. Sample vector magnitude illustrated in upper-right corner. (c) River fluxes (kg m$^{-1}$ s$^{-1}$) for July 1991, 1994, and 1995. Sample vector magnitude illustrated in upper-right corner. (d) Broad fluxes (kg m$^{-1}$ s$^{-1}$) for July 1991, 1994, and 1995. Sample vector magnitude illustrated in upper-right corner.
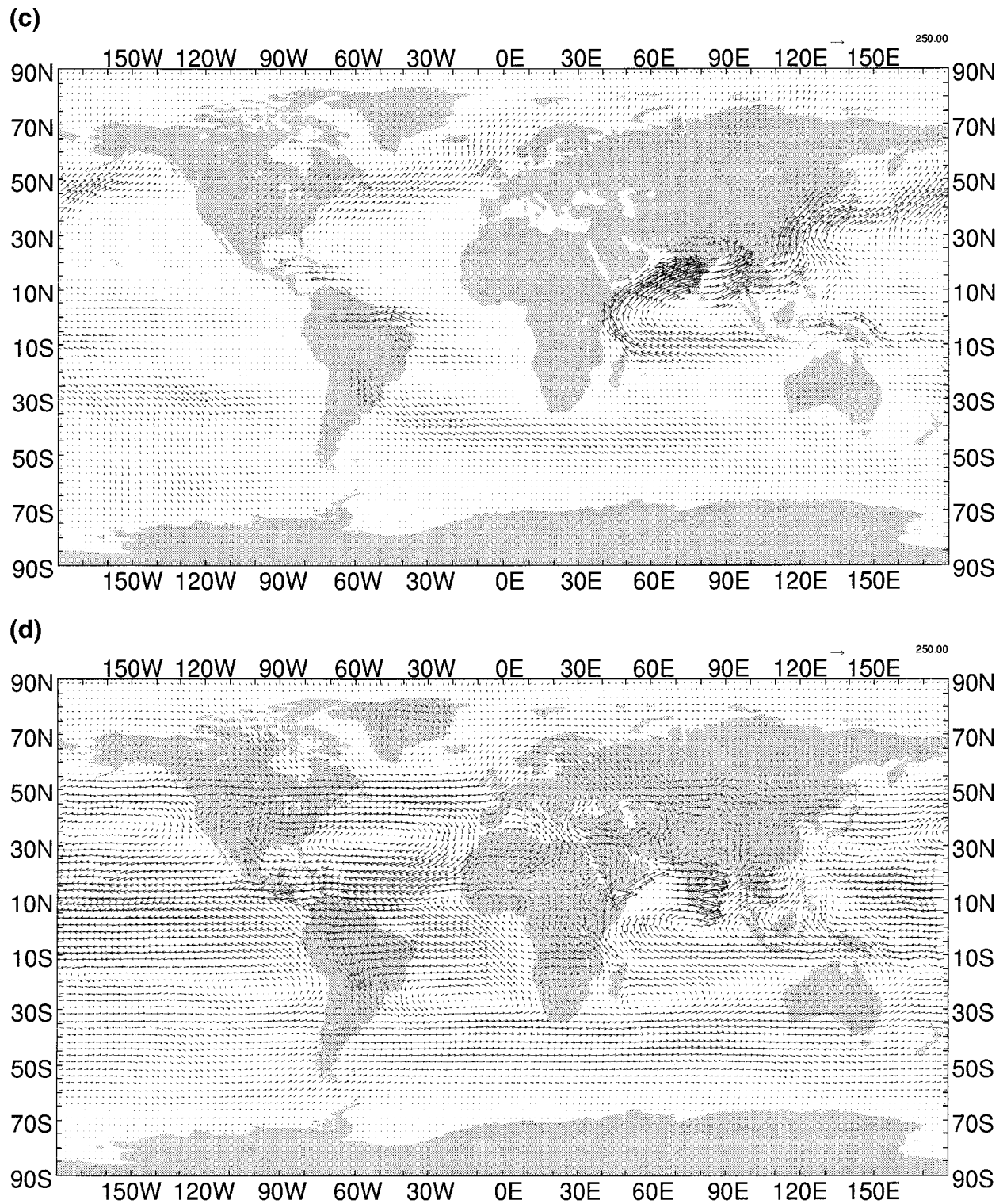
**(c)**



**(d)**



Fig. 5. (*Continued*)

## 4. Three-year statistics

The feature of river fluxes shown in Figs. 2 and 3 is a fairly common occurrence. Figure 5 illustrates the variation between January and July of the two types of flux, using gridpoint data from three 1-month periods. The river fluxes in January 1992, 1995, and 1996 (Fig. 5a) show concentrations in the central North and South Atlantic, the eastern North Pacific, and the southeast Pacific, while in July 1991, 1994, and 1995 (Fig. 5c), they also cover the Indian Ocean and Southeast Asia monsoon region. A comparison of Figs. 1b and 5c, which cover the same 3 months of July data, shows that the transient rivers formulation includes the strong convergence over western India, which is assigned to the mean fluxes in the traditional approach (Fig. 1b). Figures 5a and 5c also show a general correspondence with the storm tracks, particularly over the oceans in winter. The broad fluxes (Figs. 5b for January and 5d for July), by the selection of Eq. (11), do not show filamentary structure. Interestingly, the broad fluxes (Fig. 5d) show convergence in the Bay of Bengal in the same region that the river fluxes show divergence. This interaction is being further investigated with a series of daily maps. Figure 6 summarizes the meridional fluxes by the two types over a period of 3 years, from June 1991 to May 1992 and June 1994 to May 1996, and includes the zonal scale as in Fig. 3c. Except in the tropical regions, the seasonal and annual mean poleward transports were accomplished by rivers covering only 10% of the longitude. The relative contribution of rivers was slightly larger in the summer hemisphere than in the winter hemisphere. There is substantial interhemispheric transport in the Tropics.

Both the river and broad fluxes contributed to the interhemispheric transport in the tropical regions. The river fluxes at low latitudes may not be related to baroclinic perturbations, but to large-scale convergence in boundary regions such as the intertropical convergence zone. Since humidity contrasts were relatively weaker in tropical and subtropical regions, the rivers therein were not so strong and narrow as the extratropical rivers. The contribution of the tropical rivers to the interhemispheric transport was smaller than that of tropical broad fluxes, but could not be ignored.

## 5. Concluding comments

Instead of the Reynold's (1894)–type eddy resolution usually used for atmospheric moisture transports, we suggest here a different formulation that takes into account the filamentary structures termed atmospheric rivers. With this formulation, the rivers seem to account for a substantial fraction of the total moisture transport; in fact, for meridional transport at middle latitudes, the rivers account for substantially all of the transport. The filamentary structures are often known as conveyor belts in the synoptic literature (e.g.,
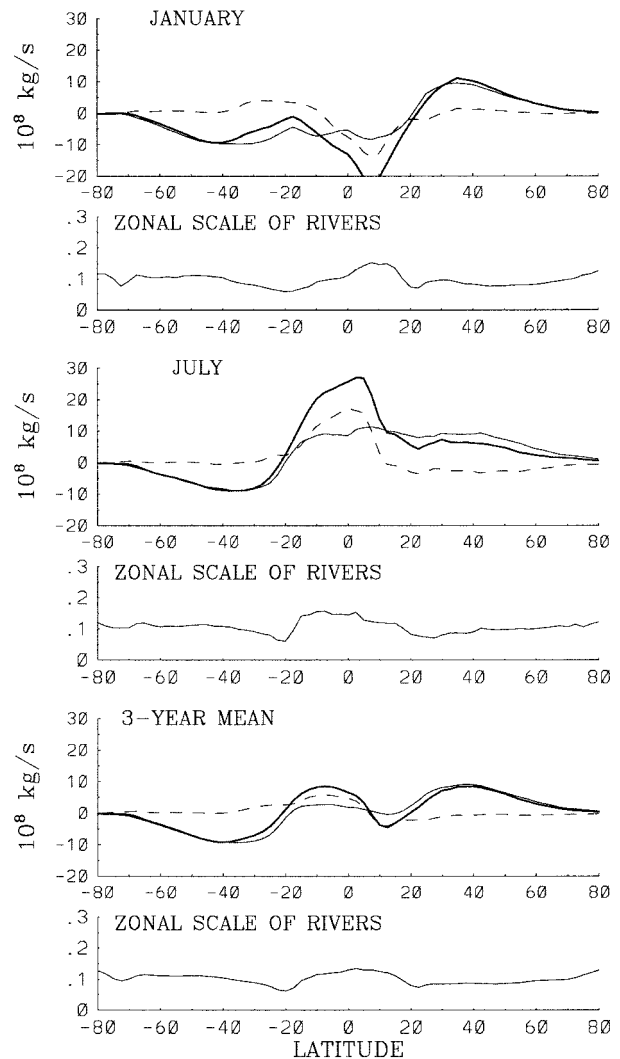


Fig. 6. Northward moisture flux by rivers, broad fluxes, and their totals. Rivers, thin solid line; broad fluxes, dashed line; and total flux, thick solid line. Units are $10^8$ kg s$^{-1}$. (Top panel) January 1992, 1995, and 1996; (second panel) zonal scale of rivers for January 1992, 1995, and 1996; (third panel) northward fluxes for July 1991, 1994, and 1995; (fourth panel) zonal scale of rivers for July 1991, 1994, and 1995; (fifth panel) northward fluxes for 3-yr mean of June 1991–May 1992 and June 1994–May 1996; (bottom panel) zonal scale of rivers for same 3-yr mean.

Browning 1990; Bluestein 1993). This new formulation supports the previous finding that these structures are coincident with the storm tracks. We showed elsewhere (Zhu and Newell 1994) that the systems known as atmospheric bombs are often associated with atmospheric rivers, as might be expected, as the main energy source giving rise to the rapid pressure fall is latent heat liberation. This liberation is maximized when a moisture filament is drawn into a developing cyclonic circulation. The formulation also showed that the majority of the middle-latitude moisture flux occurs in the filamentary features, the rivers, and that the frac-

tion of the globe they cover is 10% or less. In the Tropics, the filaments seem to arise along old cold fronts, and though their role there in total moisture transport may be small, their presence may be related systematically to the broad fluxes in ways we have currently under investigation. The fraction of the total water vapor transport assigned to moving systems may be different when the river concept is applied. It may be of practical use to track the filamentary structures on a day-to-day basis while forecasting, for as we showed elsewhere, the moisture flux convergence at the head of a river and its associated latent heat liberation is closely related to rapidly developing cyclones. The initial formation of the rivers is being modeled in association with cold frontal structures by one of our colleagues.

## REFERENCES

Bluestein, H. B., 1993: *Synoptic–Dynamic Meteorology in Midlatitudes: Volume II, Observations and Theory of Weather Systems.* Oxford University Press, 594 pp.

Browning, K. A., 1990: Organization of clouds and precipitation in extratropical cyclones. *Extratropical Cyclones: The Erik Palmen Memorial Volume,* C. W. Newton and E. O. Holopainen, Eds., Amer. Meteor. Soc., 129–153.

Newell, R. E., and Y. Zhu, 1994: Tropospheric rivers: A one-year record and a possible application to ice core data. *Geophys. Res. Lett.,* **21,** 113–116.

——, N. E. Newell, Y. Zhu, and C. Scott, 1992: Tropospheric rivers?—A pilot study. *Geophys. Res. Lett.,* **19,** 2401–2404.

Peixoto, J. P., and A. H. Oort, 1992: *Physics of Climate.* Amer. Inst. Phys. 520 pp.

Reynolds, O., 1894: On the dynamical theory of turbulent incompressible viscous fluids and the determination of the criterion. *Philos. Trans. Roy. Soc. London,* **186A,** 123–161.

Starr, V. P., and R. M. White, 1952a: Note on the seasonal variation of the meridional flux of angular momentum. *Quart. J. Roy. Meteor. Soc.,* **78,** 62–69.

——, and ——, 1952b: Schemes for the study of hemispheric exchange processes. *Quart. J. Roy. Meteor. Soc.,* **78,** 407–410.

——, and J. P. Peixoto, 1971: Pole-to-pole eddy transport of water vapor in the atmosphere during the IGY. *Arch. Meteor. Geophs. Biokl.,* **20A,** 85–114.

Zhu, Y., and R. E. Newell, 1994: Atmospheric rivers and bombs. *Geophys. Res. Lett.,* **21,** 1999–2002.